

MINIMAL INVARIANT REGIONS AND MINIMAL GLOBALLY ATTRACTING REGIONS FOR VARIABLE-K REACTION SYSTEMS

YIDA DING

Department of Mathematics, University of Wisconsin-Madison United States of America

ABHISHEK DESHPANDE* AND GHEORGHE CRACIUN

Center for Computational Natural Sciences and Bioinformatics International Institute of Information Technology Hyderabad, India Department of Mathematics and Department of Biomolecular Chemistry University of Wisconsin-Madison, United States of America

(Communicated by Sigurður Freyr Hafstein)

ABSTRACT. The structure of invariant regions and globally attracting regions is fundamental to understanding the dynamical properties of reaction network models. We describe an explicit construction of the minimal invariant regions and minimal globally attracting regions for dynamical systems consisting of two reversible reactions, where the rate constants are allowed to vary in time within a bounded interval.

1. **Introduction.** Reaction networks are ubiquitous in several mathematical models arising in biology, physics and chemistry. These models often incorporate differential equations with polynomial or power-law right hand sides [18] of the form given by

$$\frac{d\boldsymbol{x}}{dt} = \sum_{i=1}^{m} k_i \boldsymbol{x}^{\boldsymbol{s}_i} \boldsymbol{v}_i \tag{1}$$

where $\mathbf{x} = (x_1, x_2, ..., x_n) \in \mathbb{R}^n$, $\mathbf{s}_i, \mathbf{v}_i \in \mathbb{R}^n$, and $\mathbf{x}^{\mathbf{y}} := x_1^{y_1} x_2^{y_2} ... x_n^{y_n}$.

Associated with such dynamical systems is a property called *persistence* which implies that no species can go extinct, i.e., $\liminf x_i(t) > 0$ for all i. The property of persistence is related to some of the most important open problems in reaction network theory, such as the *Persistence Conjecture* and the *Global Attractor Conjecture*. Several special cases of these conjectures have been proved in the last few years, but many important problems are still open [2, 9, 12, 15]. It is therefore important to analyze invariant regions and globally attracting regions for these systems.

In general rate constants associated with reactions can vary in some range due to the change in environment like the change in pressure, temperature or external

 $^{2020\} Mathematics\ Subject\ Classification.$ Primary: 37N25, 80A30; Secondary: 92C45, 92E20, 14M25.

Key words and phrases. Persistence, permanence, invariant regions, globally attracting regions. *Corresponding author: Abhishek Deshpande.

signals, etc. Mathematically, this means that the rate constants $k_i(t)$ are functions of time. In particular, if we set constraints on the rate constants to lie in a bounded interval, these systems are called variable-k dynamical systems. For example, consider the following network

$$Y = \frac{k_1(t)}{k_2(t)} 2X$$

$$X = \frac{k_3(t)}{k_4(t)} 2Y$$
(2)

If the rate constants satisfy $\epsilon \leq k_1(t), k_2(t), k_3(t), k_4(t) \leq \frac{1}{\epsilon}$, then the dynamical systems generated by networks like (2) are called variable-k dynamical systems. In this paper, we give an explicit construction of the minimal invariant regions and minimal globally attracting regions for variable-k dynamical systems generated by two dimensional reversible reaction networks similar to network (2) described above.

This paper is structured as follows: In Section 2, we introduce the notions of persistence, permanence and uncertainty regions. In Section 3, we formally define the notions of minimal invariant regions and the minimal globally attracting regions for our dynamical systems. In Section 4, we give an explicit construction of the minimal invariant region and the minimal globally attracting region for two dimensional variable-k dynamical systems.

2. **E-graphs, Persistence and Permanence.** A reaction network is a directed graph $\mathcal{G} = (V, E)$, with a finite set of vertices $V \subset \mathbb{R}^n$ and a set of edges $E \subset V \times V$. Such a graph is also called an Euclidean embedded graph (or E-graph) [5]. If there is an edge from the vertex \mathbf{y} to the vertex \mathbf{y}' in an E-graph, we will also denote this by the reaction $\mathbf{y} \to \mathbf{y}'$ (i.e, the reactions are just the edges of \mathcal{G}). We will say that an E-graph $\mathcal{G} = (V, E)$ is reversible if for every edge $\mathbf{y} \to \mathbf{y}'$, there exists an edge $\mathbf{y}' \to \mathbf{y}$. We will say that an E-graph is weakly reversible if every edge is part of a cycle. The reaction vector of a reaction $\mathbf{y} \to \mathbf{y}'$ is the vector $\mathbf{y}' - \mathbf{y}$. The span of the reaction vectors is the stoichiometric subspace S of \mathcal{G} , i.e., it is given by $S = \{ \operatorname{span}(\mathbf{y}' - \mathbf{y}) \mid \mathbf{y} \to \mathbf{y}' \in E \}$. If we fix some $\mathbf{x}_0 \in \mathbb{R}^n_{>0}$ then the stoichiometric compatibility class (denoted by \mathcal{C}) corresponding to \mathbf{x}_0 is given by $\mathcal{C} = (\mathbf{x}_0 + S) \cap \mathbb{R}^n_{>0}$.

Every reaction network generates a family of dynamical systems on the positive orthant. If we assume mass-action kinetics [1, 21, 22, 13, 23], the dynamical systems generated by a reaction network are given by

$$\frac{dx}{dt} = \sum_{\mathbf{y} \to \mathbf{y}' \in E} k_{\mathbf{y} \to \mathbf{y}'} x^{\mathbf{y}} (\mathbf{y}' - \mathbf{y})$$
(3)

where $k_{y\to y'}>0$ is the rate constant of the reaction $y\to y'$. In general, rate constants can be time-dependent to accommodate the uncertainty introduced by external influences. In this case, the reaction network generates non-autonomous dynamical systems given by

$$\frac{dx}{dt} = \sum_{\mathbf{y} \to \mathbf{y}' \in E} k_{\mathbf{y} \to \mathbf{y}'}(t) \mathbf{x}^{\mathbf{y}}(\mathbf{y}' - \mathbf{y})$$
(4)

In particular, if the rate constants corresponding to the reactions are allowed to take values in the bounded interval $[\epsilon, \frac{1}{\epsilon}]$ for some $\epsilon > 0$, then the dynamical systems they generate are called *variable-k dynamical systems* [9, 4].

We now define some important dynamical properties of reaction networks.

Definition 2.1 (Persistence). Consider a dynamical system of the form (4). This dynamical system is said to be *persistent* if for any initial condition $x(0) \in \mathbb{R}^n_{>0}$, the solution x(t) of (4) satisfies

$$\liminf_{t \to T_{\text{max}}} \boldsymbol{x}_i(t) > 0$$
(5)

for all i = 1, 2, ..., n where T_{max} is the maximal time for which the solution exists.

Definition 2.2 (Permanence). Consider a dynamical system of the form (4). This dynamical system is said to be *permanent* if for each stoichiometric compatibility class \mathcal{C} , there exists a compact set $\mathcal{D} \subseteq \mathcal{C}$ and a time T > 0 such that for any solution $\boldsymbol{x}(t)$ of (4) with $\boldsymbol{x}(0) \in \mathcal{C}$, we have $\boldsymbol{x}(t) \in \mathcal{D}$ for all $t \geq T$.

Definition 2.3 (Detailed balance). Consider a dynamical system of the form (4) generated by a reversible E-graph $\mathcal{G} = (V, E)$. This dynamical system is said to be detailed balanced if there exists $\mathbf{x}_0 \in \mathbb{R}^n_{>0}$ such that the following holds for every reversible reaction $\mathbf{y} \rightleftharpoons \mathbf{y}' \in E$:

$$k_{\mathbf{y}\to\mathbf{y}'}\mathbf{x}_0^{\mathbf{y}} = k_{\mathbf{y}'\to\mathbf{y}}\mathbf{x}_0^{\mathbf{y}'}. \tag{6}$$

Definition 2.4 (Complex balance). Consider a dynamical system of the form (4) generated by an E-graph $\mathcal{G} = (V, E)$. This dynamical system is said to be *complex balanced* if there exists $\boldsymbol{x}_0 \in \mathbb{R}^n_{>0}$ such that the following holds for every vertex $\boldsymbol{y} \in V$:

$$\sum_{\boldsymbol{y} \to \boldsymbol{y}' \in E} k_{\boldsymbol{y} \to \boldsymbol{y}'} \boldsymbol{x}_0^{\boldsymbol{y}} = \sum_{\boldsymbol{y}' \to \boldsymbol{y} \in E} k_{\boldsymbol{y}' \to \boldsymbol{y}} \boldsymbol{x}_0^{\boldsymbol{y}'}.$$
 (7)

In what follows, we state some of the most important open problems in reaction network theory [9]:

- 1. **Persistence conjecture:** Any dynamical system generated by a weakly reversible E-graph is persistent.
- 2. Extended Persistence conjecture: Any variable-k dynamical system generated by an endotactic E-graph is persistent.
- 3. **Permanence conjecture:** Any dynamical system generated by a weakly reversible E-graph is permanent.
- 4. Extended Permanence conjecture: Any variable-k dynamical system generated by an endotactic E-graph is permanent.

labeled above conjectures are very closely related to the Global Attractor Conjecture, which states that complex balanced dynamical systems have a globally attracting fixed point [8]. In particular, the proof of any one of these four conjectures would also imply a proof of the Global Attractor Conjecture [8, 19, 20]. Several special cases of these conjectures have been proved. Craciun, Nazarov and Pantea [9] have proved the extended permanence conjecture in two dimensions. This has been extended by Pantea [15] to the case of E-graphs with two dimensional stoichiometric subspace. Anderson [2] has proved the Global Attractor Conjecture for E-graphs consisting of a single connected component. Gopalkrishnan, Miller and Shiu [12] have shown that variable-k dynamical systems generated by strongly endotactic E-graphs are permanent. A fully general proof of the Global Attractor Conjecture has recently been proposed by Craciun [4]. An essential component of the proof relies on building invariant regions for certain dynamical systems. In this

paper, we give an explicit construction of the minimal invariant regions and minimal globally attracting regions for variable-k dynamical systems generated by two reversible reactions.

Definition 2.5 (Uncertainty region). Consider the reversible reaction

$$aX + bY \xrightarrow[k_2(t)]{k_2(t)} a'X + b'Y \tag{8}$$

Now consider the variable-k dynamical systems generated by this reversible reaction if we choose rate constants as follows:

- 1. $k_1(t) = \epsilon$ and $k_2(t) = \frac{1}{\epsilon}$.
- 2. $k_1(t) = \frac{1}{\epsilon}$ and $k_2(t) = \epsilon$.

The condition for these dynamical systems to be detailed balanced gives the curves $y^{b'-b}=\epsilon^2 x^{a-a'}$ and $y^{b'-b}=\frac{1}{\epsilon^2} x^{a-a'}$ respectively. The uncertainty region corresponding to the reaction (8) is the region enclosed between the curves $y^{b'-b}=\epsilon^2 x^{a-a'}$ and $y^{b'-b}=\frac{1}{\epsilon^2} x^{a-a'}$.

Definition 2.6 (Attracting directions of an uncertainty region). Consider an uncertainty region corresponding to the reaction given by

$$aX + bY \xrightarrow[k_2(t)]{k_1(t)} a'X + b'Y \tag{9}$$

Note that this uncertainty region divides the positive orthant into three connected components, as shown in Figure 1. For components that lie outisde the uncertainty region, the attracting direction is the direction perpendicular to the line (b'-b)y = (a'-a)x and points towards this uncertainty region. Within the uncertainty region, the attracting direction is perpendicular to the line (b'-b)y = (a'-a)x (i.e. parallel to the reaction vector). The exact direction will be determined by the choice of rate constants in (9).

Remark 1. It is easy to see in Figure 1 that, for networks that consist of a <u>single</u> reversible reaction, the blue regions are *minimal globally attracting regions*. Moreover, any line segment obtained as the intersection between a blue region and a stoichiometric compatibility class is a *minimal invariant region*. Our goal in this paper is to solve this problem for the simplest nontrivial case: the case of <u>two</u> reversible reactions.

3. Variable-k reaction systems given by two reversible reactions. Consider the reaction network \mathcal{G} that consists of two reversible reactions:

$$a_1X + b_1Y \rightleftharpoons a'_1X + b'_1Y$$

$$a_2X + b_2Y \rightleftharpoons a'_2X + b'_2Y$$
(10)

for some choice of real numbers $a_1, a'_1, b_1, b'_1, a_2, a'_2, b_2, b'_2 \ge 0$.

Remark 2. In Definition 2.1 we introduced the maximal time of existence T_{max} for a solution of a dynamical system. In this paper our focus is on dynamical systems generated by two reversible reactions. For such systems the solutions are bounded and exist for all time, i.e., $T_{\text{max}} = \infty$ [9].

In what follows, we will denote by $\mathcal{G}_{\epsilon}^{\text{variable-k}}$ the set of all variable-k dynamical systems generated by \mathcal{G} . Also, if $\boldsymbol{x}(t)$ is a solution of a dynamical system contained in $\mathcal{G}_{\epsilon}^{\text{variable-k}}$, then we simply say that $\boldsymbol{x}(t)$ is a solution of $\mathcal{G}_{\epsilon}^{\text{variable-k}}$.

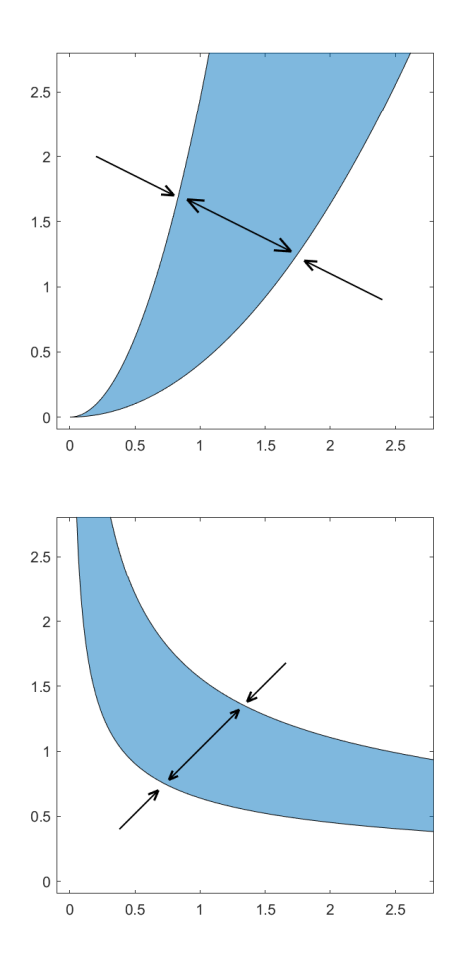


FIGURE 1. Attracting directions corresponding to the uncertainty region of a reversible reaction. On the left we show the case where the reaction has *negative* slope, and on the right we show the case where the reaction has *positive* slope.

Remark 3. We will assume that the rate constant functions $k_i(t)$ in Equation 4.1 are piecewise continuous functions of time (i.e., the set of discontinuities is a discrete set of points $t_1 < t_2 < ... < t_k < ...$, such that k_i is continuous on any interval of the form (t_k, t_{k+1}) and all the side-limits exist.) In particular, this implies that the solutions $\boldsymbol{x}(t)$ of $\mathcal{G}_{\epsilon}^{\text{variable-k}}$ depend continuously on their initial conditions.

Definition 3.1. Let $\boldsymbol{x}(t)$ be a solution of $\mathcal{G}^{\text{variable-k}}_{\epsilon}$ with initial condition $\boldsymbol{x}(0) \in \mathbb{R}^n_{>0}$. The *omega-limit* of this solution is the set $\omega(\boldsymbol{x}(t)) = \{\boldsymbol{z} \in \mathbb{R}^n_{\geq 0} : \text{there is an increasing sequence of times } (t_h)_{h \in \mathbb{N}} \text{such that } \lim_{h \to \infty} t_h = \infty \text{ and } \lim_{h \to \infty} \boldsymbol{x}(t_h) = \boldsymbol{z} \}.$

Definition 3.2. A set $\Omega_{\text{variable-k}}^{\text{inv}} \in \mathbb{R}^n_{>0}$ is said to be a *closed invariant region* of $\mathcal{G}^{\text{variable-k}}_{\epsilon}$ if it is closed and for any solution $\boldsymbol{x}(t)$ of $\mathcal{G}^{\text{variable-k}}_{\epsilon}$ with $\boldsymbol{x}(0) \in \Omega^{\text{inv}}_{\text{variable-k}}$, we have $\boldsymbol{x}(t) \in \Omega^{\text{inv}}_{\text{variable-k}}$ for all t > 0. A set $\Omega^{\text{min,inv}}_{\text{variable-k}}$ is said to be the *minimal closed invariant region* of $\mathcal{G}^{\text{variable-k}}_{\epsilon}$ if for any closed invariant region $\Omega_{\text{variable-k}}$, we

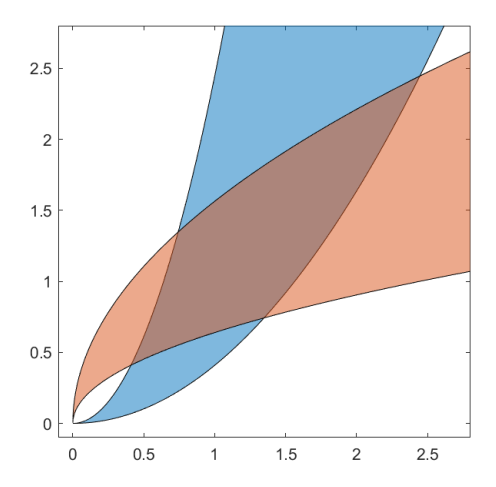


Figure 2. An example of uncertainty regions corresponding to the reaction network described in (10). Here we illustrate the case where the slopes of both reaction vectors are negative. We will always represent in red the uncertainty region of the reaction $a_1X +$ $b_1Y \xrightarrow[k_2(t)]{k_1(t)} a'_1X + b'_1Y$, and in blue the uncertainty region of the reaction $a_2X + b_2Y \xrightarrow[k_4(t)]{k_3(t)} a'_2X + b'_2Y$.

have $\Omega_{\text{variable-k}}^{\text{min,inv}} \subseteq \Omega_{\text{variable-k}}$. For simplicity, instead of minimal closed invariant region we will simply say minimal invariant region.

Definition 3.3. A set $\Omega^{\text{glob}}_{\text{variable-k}} \in \mathbb{R}^n_{>0}$ is said to be a *globally attracting region* of $\mathcal{G}^{\text{variable-k}}_{\epsilon}$ if for any solution $\boldsymbol{x}(t)$ of $\mathcal{G}^{\text{variable-k}}_{\epsilon}$ with $\boldsymbol{x}(0) \in \mathbb{R}^n_{>0}$, we have $\omega(\boldsymbol{x}(t)) \subseteq \Omega^{\text{glob}}_{\text{variable-k}}$. A set $\Omega^{\min,\text{glob}}_{\text{variable-k}}$ is said to be the *minimal globally attracting region* of $\mathcal{G}^{\text{variable-k}}_{\epsilon}$ if for any globally attracting region $\Omega_{\text{variable-k}}$, we have $\Omega^{\min,\text{glob}}_{\text{variable-k}} \subseteq \Omega^{\min,\text{glob}}_{\epsilon}$ $\Omega_{\text{variable-k}}^{\text{glob}}$.

Definition 3.4. Given two points $P, Q \in \mathbb{R}^n_{>0}$, we say $P \leadsto Q$ if there is a solution x(t) of $\mathcal{G}^{\text{variable-k}}_{\epsilon}$ such that x(0) = P and for every $\xi > 0$ there exists a T that satisfies $||x(T) - Q|| \le \xi$.

- 4. Minimal invariant region and minimal globally attracting region for variable-k dynamical systems generated by two reversible reactions. According to how we choose the parameters $a_1, a'_1, b_1, b'_1, a_2, a'_2, b_2, b'_2$, we get the following cases that correspond to various configurations of the uncertainty regions.
- (i) Both reaction vectors with negative slopes; one with slope less than -1 and the other with slope greater than -1: $-1 < \frac{b'_1 - b_1}{a'_1 - a_1} < 0$ and $\frac{b'_2 - b_2}{a'_2 - a_2} < -1$.

 (ii) Both reaction vectors with slopes between 0 and -1: $-1 < \frac{b'_1 - b_1}{a'_1 - a_1}, \frac{b'_2 - b_2}{a'_2 - a_2} < 0$.

 (iii) Both reaction vectors with slopes less than -1: $\frac{b'_1 - b_1}{a'_1 - a_1} < -1$ and $\frac{b'_2 - b_2}{a'_2 - a_2} < -1$.

- (iv) Both reaction vectors with positive slopes: $\frac{b_1'-b_1}{a_1'-a_1} > 0$ and $\frac{b_2'-b_2}{a_2'-a_2} > 0$.

- (v) One reaction vector with positive slope and the other with slope between -1
- (vi) One reaction vector with positive slope and the other with slope less than -1: $and 0: \frac{b'_2 b_2}{a'_2 a_2} > 0 \text{ and } -1 < \frac{b'_1 b_1}{a'_1 a_1} < 0.$ (vi) One reaction vector with positive slope and the other with slope less than -1: $\frac{b'_2 b_2}{a'_2 a_2} > 0 \text{ and } \frac{b'_1 b_1}{a'_1 a_1} < -1.$

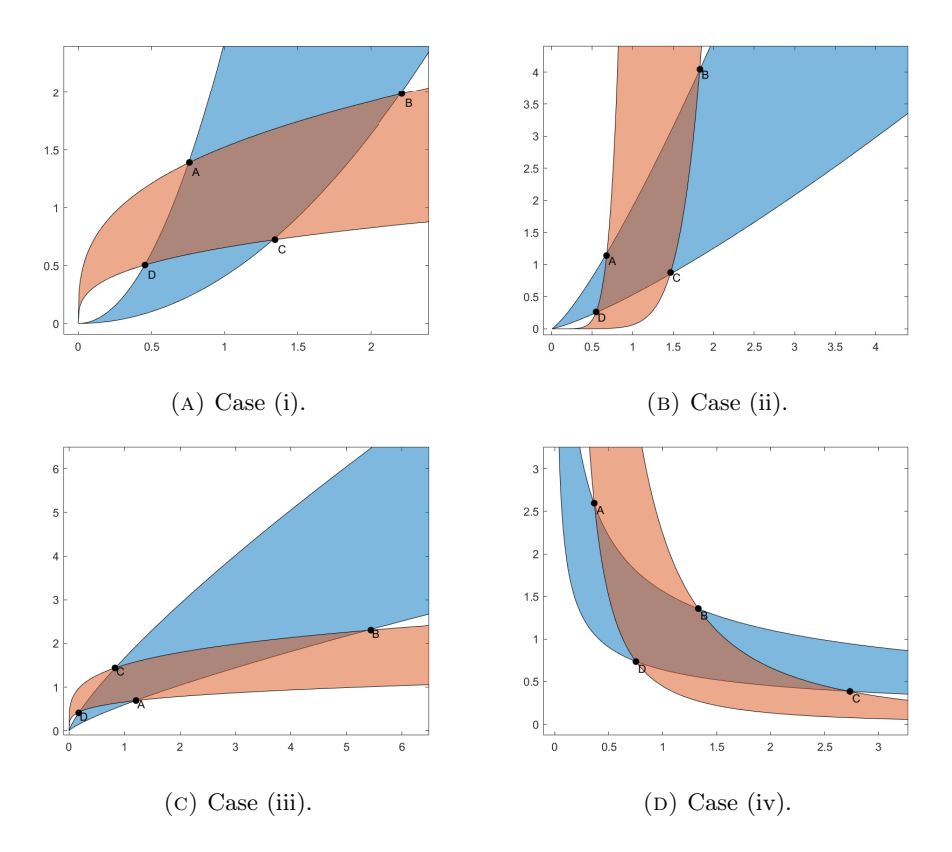


FIGURE 3. Uncertainty regions corresponding to two reversible reactions in case (i)-(iv).

Figure 3 illustrates the uncertainty regions corresponding to cases (i)-(iv). Throughout this paper, the analysis for cases (i)-(iv) will be similar, while, for simplicity, in cases (v) and (vi) we will make the additional assumption that ϵ is small enough. In subsection 4.1 we will discuss how to construct the minimal invariant region and minimal globally attracting region for cases (i)-(iv). For simplicity, we will only consider case (i), i.e. both reaction vectors with negative slopes; one with slope less than -1 and the other with slope greater than -1: $-1 < \frac{b_1' - b_1}{a_1' - a_1} < 0$ and $\frac{b_2'-b_2}{a_2'-a_2} < -1$; the analysis for other cases will proceed analogously. Throughout the next subsection, all references to the dynamical system will be with respect to

4.1. Cases (i)-(iv). In the following lemma we show that fixing the rate constants to certain values also fixes the omega-limit points of the trajectories corresponding to the variable-k dynamical system generated by two reversible reactions.

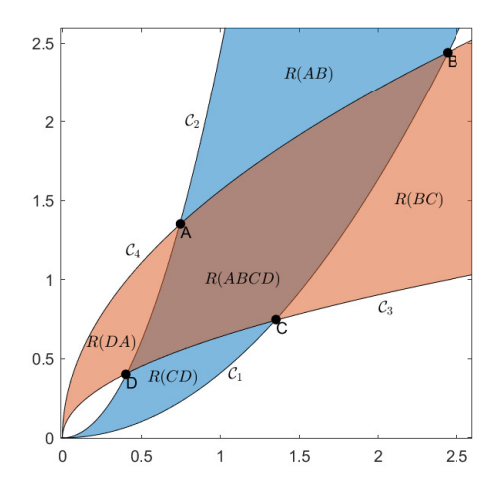


FIGURE 4. Uncertainty regions corresponding to two reversible reactions. Regions R_{AB} , R_{BC} , R_{CD} , R_{DA} , R_{ABCD} are also marked on the figure. Note that the curves C_1 and C_2 are interchangeable, depending on the sign of $a'_1 - a_1$; similarly the curves C_3 and C_4 are interchangeable, depending on the sign of $b'_1 - b_1$.

Lemma 4.1. Consider the dynamical systems in $\mathcal{G}_{\epsilon}^{\text{variable-k}}$, and consider the following curves (see Fig. 4 for an example):

$$\begin{array}{l} \mathcal{C}_1: x^{a'_1-a_1}y^{b'_1-b_1} = \frac{1}{\epsilon^2}.\\ \mathcal{C}_2: x^{a'_1-a_1}y^{b'_1-b_1} = \epsilon^2.\\ \mathcal{C}_3: x^{a'_2-a_2}y^{b'_2-b_2} = \epsilon^2.\\ \mathcal{C}_4: x^{a'_2-a_2}y^{b'_2-b_2} = \frac{1}{\epsilon^2}. \end{array}$$

Let A be the intersection point of the curves C_2 and C_4 , B be the intersection point of the curves C_1 and C_4 , C be the intersection point of the curves C_1 and C_3 and D be the intersection point of the curves C_2 and C_3 . Denote by $\mathbf{x}(t)$ any solution of $G_{\epsilon}^{\text{variable-k}}$ with $\mathbf{x}(0) \in \mathbb{R}^2_{>0}$. Then we have the following:

(i) If
$$k_1(t) = \epsilon$$
, $k_2(t) = \frac{1}{\epsilon}$, $k_3(t) = \frac{1}{\epsilon}$, $k_4(t) = \epsilon$ for all t , then $\lim_{t \to \infty} \boldsymbol{x}(t) = A$.

(ii) If
$$k_1(t) = \frac{1}{\epsilon}$$
, $k_2(t) = \epsilon$, $k_3(t) = \frac{1}{\epsilon}$, $k_4(t) = \epsilon$ for all t , then $\lim_{t \to \infty} x(t) = B$.

(iii) If
$$k_1(t) = \frac{1}{\epsilon}$$
, $k_2(t) = \epsilon$, $k_3(t) = \epsilon$, $k_4(t) = \frac{1}{\epsilon}$ for all t , then $\lim_{t \to \infty} \boldsymbol{x}(t) = C$.

(iv) If
$$k_1(t) = \epsilon$$
, $k_2(t) = \frac{1}{\epsilon}$, $k_3(t) = \epsilon$, $k_4(t) = \frac{1}{\epsilon}$ for all t , then $\lim_{t \to \infty} \boldsymbol{x}(t) = D$.

Proof. In case (i), note that the point A is the intersection of the curves $x^{a_1'-a_1}y^{b_1'-b_1} = \frac{1}{\epsilon^2}$ and $x^{a_2'-a_2}y^{b_2'-b_2} = \frac{1}{\epsilon^2}$. If $k_1(t) = \frac{1}{\epsilon}$, $k_2(t) = \epsilon$, $k_3(t) = \frac{1}{\epsilon}$, $k_4(t) = \epsilon$, then the point A becomes a detailed balanced equilibrium, since $k_1(t)x^{a_1}y^{b_1} = k_2(t)x^{a_1'}y^{b_1'}$ and $k_3(t)x^{a_2}y^{b_2} = k_4(t)x^{a_2'}y^{b_2'}$. Then it follows from [9] that $\lim_{t\to\infty} x(t) = A$. The other cases are analogous.

Constructing the set \mathcal{M}_{ϵ} . Consider the intersection points A, B, C, D as described in Lemma 4.1. Figure 4 illustrates these points. Since we are only dealing

with cases (i)-(iv) as described in Section 4.1 (where the slopes of both reaction vectors have the same sign), the uncertainty regions corresponding to the two reversible reactions are as described in Figure 3. In cases (i)-(iii), the attracting directions at points A, B, C, D have negative slopes; on the other hand, the tangents to the curves C_1, C_2, C_3, C_4 at points A, B, C, D all have positive slopes. Therefore the cone formed by the attracting directions at points B and D contains the region R_{ABCD} , while the cone formed by the attracting directions at points A and C is contained in the region R_{ABCD} . In case (iv), the cone formed by the attracting directions at points B and D is contained in the region R_{ABCD} ; while the cone formed by the attracting directions at points B and B is contained in the region B is contained in the re

Starting from points B and D we construct four special trajectory curves, by choosing rate constants such that the points A and C become globally attracting points (like in Lemma 4.1 (i) and (iii)). The region enclosed by these four trajectories is \mathcal{M}_{ϵ} (see Fig. 5).

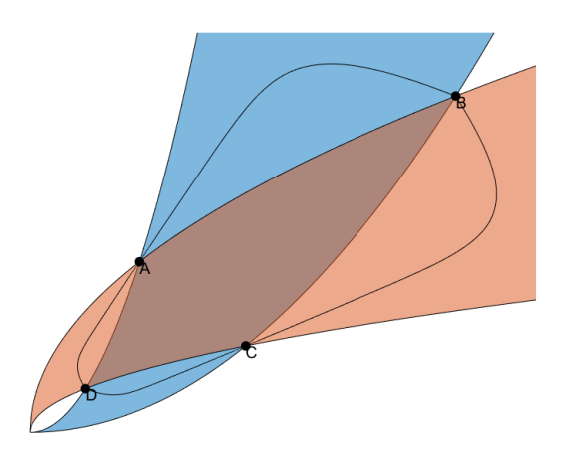


FIGURE 5. We will prove that the minimal invariant region and the minimal globally attracting region of $\mathcal{G}_{\epsilon}^{\text{variable}-k}$ is given by the set \mathcal{M}_{ϵ} enclosed by the trajectory curves starting from B and D and converging to the points A and C.

Proposition 1. We have $\mathcal{M}_{\epsilon} \subset R_{AB} \cup R_{BC} \cup R_{CD} \cup R_{DA} \cup R_{ABCD}$.

Proof. Consider a solution x(t) of $\mathcal{G}_{\epsilon}^{\text{variable-k}}$ with x(0) = D. The dynamical system it generates is given by

$$\begin{pmatrix} \dot{x} \\ \dot{y} \end{pmatrix} = \left(k_1(t) x^{a_1} y^{b_1} - k_2(t) x^{a_1'} y^{b_1'} \right) \begin{pmatrix} a_1' - a_1 \\ b_1' - b_1 \end{pmatrix} + \\ \left(k_3(t) x^{a_2} y^{b_2} - k_4(t) x^{a_2'} y^{b_2'} \right) \begin{pmatrix} a_2' - a_2 \\ b_2' - b_2 \end{pmatrix}$$

If we choose rate constants $k_1(t) = \epsilon, k_2(t) = \frac{1}{\epsilon}, k_3(t) = \frac{1}{\epsilon}, k_4(t) = \epsilon$, then by Lemma 4.1 we get $\lim_{t\to\infty} \boldsymbol{x}(t) = A$. We now show that this trajectory stays inside the

¹Here, by the word "cone" we mean the *convex cone* generated by the two attracting directions.

region R_{DA} . Since we are in case (i), we have -1: $-1 < \frac{b'_1 - b_1}{a'_1 - a_1} < 0$ and $\frac{b'_2 - b_2}{a'_2 - a_2} < -1$. Therefore, within the region R_{DA} , the trajectory is confined to a cone formed by $\mathbf{v}_1 = \begin{pmatrix} a'_1 - a_1 \\ b'_1 - b_1 \end{pmatrix}$ and $\mathbf{v}_2 = \begin{pmatrix} a'_2 - a_2 \\ b'_2 - b_2 \end{pmatrix}$ as shown in Figure 6.

Denote by O the origin. Due to our choice of rate constants, on the curve OD the attracting direction of the blue uncertainty region is inactive. The only contribution on this curve is due to the attracting direction of the red uncertainty region, which sends the trajectory to the interior of OAD. Therefore, this trajectory cannot cross the curve OD. We show that it also cannot cross the curves OA and DA. For contradiction, assume that the trajectory intersects OA at a point P. Note that since the point P lies on the curve C_4 , we have $k_3(t)x^{a_2}y^{b_2} = k_4(t)x^{a'_2}y^{b'_2}$. Therefore, the only contribution to the vector field at the point P is due to the attracting direction of the blue uncertainty region (shown as v_1 in Figure 6) which points towards the region OAD; this contradicts our assumption that our trajectory reaches P. A similar argument shows that the trajectory cannot cross the curve DA. Repeating this for the other parts of the boundary of \mathcal{M}_{ϵ} , we get that $\mathcal{M}_{\epsilon} \subset R_{AB} \cup R_{BC} \cup R_{CD} \cup R_{DA}$, as required.

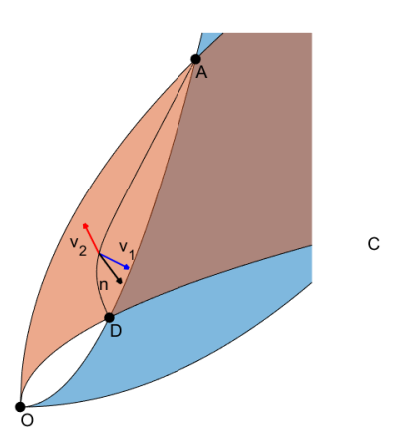


FIGURE 6. The direction of the trajectory from D to A is confined to the cone formed by vectors v_1 and v_2 . In particular, this means that this trajectory lies in the region R_{DA} (shown in light orange color).

Proposition 2. The set \mathcal{M}_{ϵ} is an invariant region for any dynamical system in $\mathcal{G}^{\text{variable-k}}_{\epsilon}$.

Proof. To show that \mathcal{M}_{ϵ} is an invariant region, it suffices to show that on the boundary of \mathcal{M}_{ϵ} , the vector field points towards the interior of \mathcal{M}_{ϵ} [14, 3]. Towards this, consider the dynamical system generated by (10)

$$\begin{pmatrix} \dot{x} \\ \dot{y} \end{pmatrix} = \left(k_1(t) x^{a_1} y^{b_1} - k_2(t) x^{a'_1} y^{b'_1} \right) \begin{pmatrix} a'_1 - a_1 \\ b'_1 - b_1 \end{pmatrix} +$$
 (11)

$$\left(k_3(t)x^{a_2}y^{b_2} - k_4(t)x^{a_2'}y^{b_2'}\right) \begin{pmatrix} a_2' - a_2 \\ b_2' - b_2 \end{pmatrix}$$
(12)

Let

$$\mathbf{v}_1 = \begin{pmatrix} a_1' - a_1 \\ b_1' - b_1 \end{pmatrix} \text{ and } \mathbf{v}_2 = \begin{pmatrix} a_2' - a_2 \\ b_2' - b_2 \end{pmatrix}.$$
 (13)

Then Equation (11) can be written as

$$\begin{pmatrix} \dot{x} \\ \dot{y} \end{pmatrix} = \left(k_1(t) x^{a_1} y^{b_1} - k_2(t) x^{a'_1} y^{b'_1} \right) \boldsymbol{v}_1 + \left(k_3(t) x^{a_2} y^{b_2} - k_4(t) x^{a'_2} y^{b'_2} \right) \boldsymbol{v}_2 \tag{14}$$

We will show that on the boundary of \mathcal{M}_{ϵ} consisting of the trajectory from D to A, the vector field points towards the interior of \mathcal{M}_{ϵ} . The proof for other parts of the boundary of \mathcal{M}_{ϵ} will follow analogously. From Lemma 4.1, the trajectory from D to A is given by the following system of ODEs.

$$\begin{pmatrix} \dot{x} \\ \dot{y} \end{pmatrix}_{D \to A} = \left(\epsilon x^{a_1} y^{b_1} - \frac{1}{\epsilon} x^{a'_1} y^{b'_1} \right) v_1 + \left(\frac{1}{\epsilon} x^{a_2} y^{b_2} - \epsilon x^{a'_2} y^{b'_2} \right) v_2$$
 (15)

(where we have used the fact that $k_1(t) = \epsilon$, $k_2(t) = \frac{1}{\epsilon}$, $k_3(t) = \frac{1}{\epsilon}$, $k_4(t) = \epsilon$). Let **n** denote the inward pointing normal to the trajectory given by Equation (15). We will show that

$$\begin{pmatrix} \dot{x} \\ \dot{y} \end{pmatrix} \cdot \mathbf{n} \ge 0 \tag{16}$$

Note that

$$\begin{pmatrix} \dot{x} \\ \dot{y} \end{pmatrix}_{D \to A} \cdot \mathbf{n} = \left[\left(\epsilon x^{a_1} y^{b_1} - \frac{1}{\epsilon} x^{a_1'} y^{b_1'} \right) \boldsymbol{v}_1 + \left(\frac{1}{\epsilon} x^{a_2} y^{b_2} - \epsilon x^{a_2'} y^{b_2'} \right) \boldsymbol{v}_2 \right] \cdot \mathbf{n} = 0$$
 (17)

Since within region OAD, the trajectory of the dynamical system is confined to the cone formed by vectors \mathbf{v}_1 and \mathbf{v}_2 (as shown in Figure 6), we get $\mathbf{v}_1 \cdot \mathbf{n} > 0$ and $\mathbf{v}_2 \cdot \mathbf{n} < 0$. Noting that $\epsilon \leq k_1(t), k_2(t), k_3(t), k_4(t) \leq \frac{1}{\epsilon}$, we have

$$\left(k_{1}(t)x^{a'_{1}}y^{b'_{1}} - k_{2}(t)x^{a_{1}}y^{b_{1}}\right)\boldsymbol{v}_{1} \cdot \mathbf{n} \ge \left(\epsilon x^{a_{1}}y^{b_{1}} - \frac{1}{\epsilon}x^{a'_{1}}y^{b'_{1}}\right)\boldsymbol{v}_{1} \cdot \mathbf{n}$$
(18)

and

$$\left(k_3(t)x^{a_2}y^{b_2} - k_4(t)x^{a_2'}y^{b_2'}\right)\mathbf{v}_2 \cdot \mathbf{n} \ge \left(\frac{1}{\epsilon}x^{a_2}y^{b_2} - \epsilon x^{a_2'}y^{b_2'}\right)\mathbf{v}_2 \cdot \mathbf{n} \tag{19}$$

Adding Equations (18) and (19) and using Equation (17), we get that

$$\left[\left(k_1(t)x^{a_1}y^{b_1} - k_2(t)x^{a'_1}y^{b'_1} \right) \boldsymbol{v}_1 + \left(k_3(t)x^{a_2}y^{b_2} - k_4(t)x^{a'_2}y^{b'_2} \right) \boldsymbol{v}_2 \right] \cdot \mathbf{n} \ge 0 \quad (20)$$

as required. \Box

Remark 4. Note that Proposition 2 shows that \mathcal{M}_{ϵ_0} is an invariant region for $\epsilon_0 > 0$. For all $\epsilon < \epsilon_0$, the inequalities given by Equations (18), (19) and (20) become strict and hence the net vector field along the boundary of \mathcal{M}_{ϵ} points strictly onto its interior.

Remark 5. Consider points $P_1, P_2, P_3 \in \mathbb{R}^2_{>0}$. If we have $P_1 \rightsquigarrow P_2$ and $P_2 \rightsquigarrow P_3$, then we have $P_1 \rightsquigarrow P_3$. This is due to the fact the rate constants are assumed to be piecewise continuous functions of time and the solutions of these dynamical systems depend continuously on their initial conditions (see Remark 3).

Proposition 3. If $P_2 \in \mathcal{M}_{\epsilon}$, then $P_1 \rightsquigarrow P_2$ for any $P_1 \in \mathbb{R}^2_{>0}$.

Proof. We proceed by case analysis. (Refer to Figures 4 and 5).

- (i) $P_2 \in R_{ABCD}$: Then P_2 is the intersection of the curves $k_2 x^{a_1} y^{b_1} = k_1 x^{a'_1} y^{b'_1}$ and $k_4 x^{a_2} y^{b_2} = k_3 x^{a'_2} y^{b'_2}$ for some constants $\epsilon \leq k_1, k_2, k_3, k_4 \leq \frac{1}{\epsilon}$. Choosing $k_1(t) = k_1, k_2(t) = k_2, k_3(t) = k_3, k_4(t) = k_4$, we get that P is detailed balanced for these choice of rate constants. Noting that the dynamical system is two-dimensional, it follows from [9] that $P_1 \rightsquigarrow P_2$.
- (ii) $P_2 \in \mathcal{M}_{\epsilon} \backslash R_{ABCD}$: Without loss of generality, assume that the point P_2 lies in the region OAD (similar arguments will work in the other regions). Consider a trajectory $\boldsymbol{x}(t)$ of this dynamical system with $\boldsymbol{x}(0) = P_1$ and choose rate constants $k_1(t) = \epsilon, k_2(t) = \frac{1}{\epsilon}, k_3(t) = \epsilon, k_4(t) = \frac{1}{\epsilon}$ as in Lemma 4.1 so that $\lim_{t\to\infty} \boldsymbol{x}(t) = D$.

Construct a line through P_2 , in the attracting direction of the blue uncertainty region. Note that the points D and A are on opposite sides of this line. Denote by Q the intersection point between this line and the curve DA. (Here the curve DA refers to one that lies on the boundary of \mathcal{M}_{ϵ}). Now starting close to D on the DA curve, choose rate constants $k_1(t) = \epsilon, k_2(t) = \frac{1}{\epsilon}, k_3(t) = \frac{1}{\epsilon}, k_4(t) = \epsilon$, so that $\lim_{t \to \infty} \boldsymbol{x}(t) = A$. Let $(\tilde{x}(t), \tilde{y}(t))$ denote this trajectory. Let T be the time when $(\tilde{x}(T), \tilde{y}(T)) = Q$. After time T, set the rate constants of the reaction corresponding to the red uncertainty region such that $k_3(t)\tilde{x}(t)^{a_2}\tilde{y}(t)^{b_2} = k_4(t)\tilde{x}(t)^{a_2'}\tilde{y}(t)^{b_2'}$. (Note that this is possible since we are in the red uncertainty region.) This means the only vector field at point Q is due to the attracting direction of the blue uncertainty region. Trace this trajectory till we get to the point P_2 . From Remark 5, we get that $P_1 \rightsquigarrow P_2$.

Theorem 4.2. The set \mathcal{M}_{ϵ} is the minimal invariant region of $\mathcal{G}_{\epsilon}^{\text{variable-k}}$.

Proof. Note that Proposition 2 shows that \mathcal{M}_{ϵ} is an invariant region for any dynamical system generated by the reaction network in Equation (10). To show that \mathcal{M}_{ϵ} is the minimal invariant region, we prove that \mathcal{M}_{ϵ} is contained in every invariant region of the dynamical system. This follows from Proposition 3 as follows. Let M be any invariant region and pick some $Z \in M$ and some $X \in \mathcal{M}_{\epsilon}$. Construct trajectories from Z that come closer and closer to X. Since M is invariant, this gives rise to points in M at arbitrarily small distance to X. Since M is closed, it follows that $X \in M$, and therefore $\mathcal{M}_{\epsilon} \subset M$.

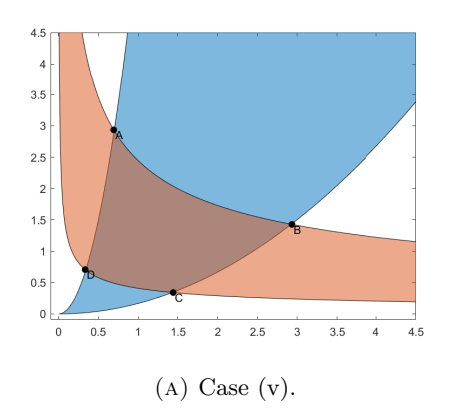
4.2. Cases (v)-(vi). The goal of this section is to construct the region \mathcal{M}_{ϵ} for cases (v) and (vi), where one reaction vector has positive slope and the other has negative slope. Figure 3 illustrates the uncertainty regions corresponding to cases (i)-(iv).

In what follows, we present the analysis of case (v); the analysis for case (vi) is completely analogous.

Consider the reaction network given in (10). The dynamical system it generates is given by

$$\begin{pmatrix} \dot{x} \\ \dot{y} \end{pmatrix} = \left(k_1(t) x^{a_1} y^{b_1} - k_2(t) x^{a_1'} y^{b_1'} \right) \begin{pmatrix} a_1' - a_1 \\ b_1' - b_1 \end{pmatrix} + \\ \left(k_3(t) x^{a_2} y^{b_2} - k_4(t) x^{a_2'} y^{b_2'} \right) \begin{pmatrix} a_2' - a_2 \\ b_2' - b_2 \end{pmatrix}$$

For convenience, we will denote $p_1 = a_1 - a'_1, q_1 = b'_1 - b_1, p_2 = a_2 - a'_2, q_2 = b'_2 - b_2$. Without loss of generality, assume that $p_1 = a_1 - a'_1 > q_1 = b'_1 - b_1 > 0$,



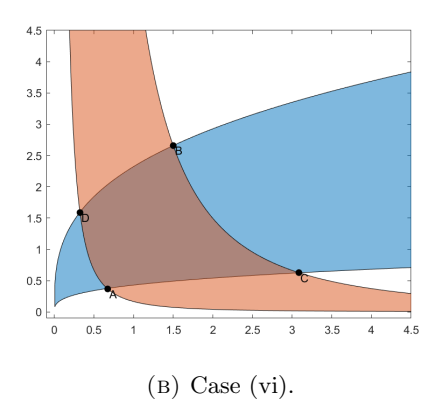


FIGURE 7. Uncertainty regions corresponding to two reversible reactions in case (v)-(vi).

 $p_2=a_2-a_2'<0,\ q_2=b_2'-b_2>0.$ Consider the following intersection points as shown in Figure 7.

- $\begin{array}{l} \text{(i)} \ \ A: y^{q_1} = \frac{1}{\epsilon^2} x^{p_1} \text{ and } y^{q_2} = \frac{1}{\epsilon^2} x^{p_2}. \\ \text{(ii)} \ \ B: y^{q_1} = \epsilon^2 x^{p_1} \text{ and } y^{q_2} = \frac{1}{\epsilon^2} x^{p_2}. \\ \text{(iii)} \ \ C: y^{q_1} = \epsilon^2 x^{p_1} \text{ and } y^{q_2} = \epsilon^2 x^{p_2}. \end{array}$
- (iv) $D: y^{q_1} = \frac{1}{\epsilon^2} x^{p_1}$ and $y^{q_2} = \epsilon^2 x^{p_2}$.

Table 1 shows the slopes of the tangents to the boundary of the uncertainty regions at their intersection points. We split our analysis into three subcases depending on the sign of $p_1 + p_2 - q_1 - q_2$.

Table 1. Slope of the tangents at the intersection of uncertainty regions in the limit $\epsilon \to 0$

$m_A^{p_1,q_1}$	$\frac{p_1}{q_1} \epsilon^{\frac{2(-p_1+p_2+q_1-q_2)}{p_1 q_2-p_2 q_1}}$
$m_A^{p_2,q_2}$	$\frac{p_2}{q_2} \epsilon^{\frac{2(-p_1+p_2+q_1-q_2)}{p_1q_2-p_2q_1}}$
$m_B^{p_1,q_1}$	$\frac{p_1}{q_1} \epsilon^{\frac{2(-p_1 - p_2 + q_1 + q_2)}{p_1 q_2 - p_2 q_1}}$
$m_B^{p_2,q_2}$	$\frac{p_2}{q_2} \epsilon^{\frac{2(-p_1 - p_2 + q_1 + q_2)}{p_1 q_2 - p_2 q_1}}$
$m_C^{p_1,q_1}$	$\frac{p_1}{q_1} \epsilon^{\frac{2(p_1 - p_2 - q_1 + q_2)}{p_1 q_2 - p_2 q_1}}$
$m_C^{p_2,q_2}$	$\frac{p_2}{q_2} \epsilon^{\frac{2(p_1 - p_2 - q_1 + q_2)}{p_1 q_2 - p_2 q_1}}$
$m_D^{p_1,q_1}$	$\frac{p_1}{q_1} \epsilon^{\frac{2(p_1 + p_2 - q_1 - q_2)}{p_1 q_2 - p_2 q_1}}$
$m_D^{p_2,q_2}$	$\frac{p_2}{q_2} \epsilon^{\frac{2(p_1 + p_2 - q_1 - q_2)}{p_1 q_2 - p_2 q_1}}$

Case (a): $p_1+p_2-q_1-q_2<0$. In this case, note that $m_D^{p_2,q_2}\to -\infty$ and $m_C^{p_2,q_2}\to 0$ as $\epsilon\to 0$. Since the slope of the tangent to the lower red curve varies continuously as we traverse from along the curve D to C, there exists a point E at which the slope of the tangent to the red curve has the same slope as the attracting direction of the blue uncertainty region. We construct trajectories of this dynamical system starting from the point E that go towards C and D. We now claim that both these trajectories stay inside the region R(CD). Figure 8 illustrates this point.

We show that the trajectory cannot cross the curve OC. For contradiction, assume that the trajectory intersects OC at point P. Note that since the point P lies on the boundary of the blue uncertainty region, the vector field at point P is given by the red attracting direction which points towards the interior of the region R_{CD} . We now show that the trajectory cannot cross the curves EC and ED. For contradiction, assume that the trajectory intersects EC at point P'. Note that the slope of the tangents to the lower red curve increase monotonically from E to C. Therefore, the net vector field at point P' which is in the blue attracting direction points towards the interior of the region R_{CD} . A similar argument can be used to show that the trajectory cannot intersect the curve ED.

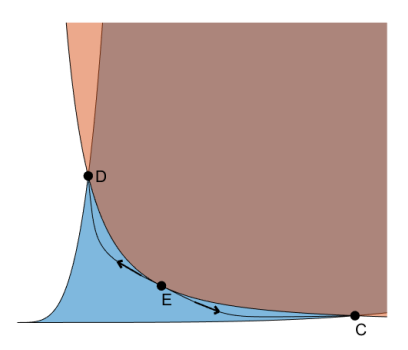


FIGURE 8. In subcase (a), there exists a point E on the curve from D to C where the slope of the tangent to the red curve has the same slope as the attracting direction of the blue uncertainty region. The boundary of \mathcal{M}_{ϵ} in this region is given by trajectories that start from E and go towards C and D.

We now show that the trajectory cannot cross the curve OD. One can calculate the coordinate of E to be the following: $x_E = \left(-\frac{q_1q_2}{p_1p_2}\right)^{\frac{q_2}{p_2-q_2}}$ $e^{-\frac{2}{p_2-q_2}}, y_E = \left(-\frac{q_1q_2}{p_1p_2}\right)^{\frac{p_2}{p_2-q_2}} e^{-\frac{2}{p_2-q_2}}$. In the discussion that follows,

please refer Figure 9. Extend the tangent at E so that it meets OD at point H. Let F be the point on the curve OD, where slope of the tangent is equal to the slope of the attracting direction corresponding to the red uncertainty region. The coordinate of F is given by the fol-

to the red uncertainty region. The coordinate of
$$F$$
 is given by the following: $x_F = \left(-\frac{q_1q_2}{p_1p_2}\right)^{\frac{q_1}{p_1-q_1}} \epsilon^{\frac{2}{p_1-q_1}}, y_F = \left(-\frac{q_1q_2}{p_1p_2}\right)^{\frac{p_1}{p_1-q_1}} \epsilon^{\frac{2}{p_1-q_1}-\frac{2}{p_1}+\frac{2}{q_1}}.$

We now show that y_F is lesser than the y-coordinate of the point H. Since $p_1 + p_2 - q_1 - q_2 < 0$ and $p_1 > q_1$, we have $-\frac{2}{p_2 - q_2} < \frac{2}{p_1 - q_1} < \frac{2}{p_1 - q_1} - \frac{2}{p_1} + \frac{2}{q_1}$. Therefore, we get $y_F - (-\frac{q_1}{p_1})x_F - [y_E - (-\frac{q_1}{p_1})x_E] = \frac{1}{p_1}[p_1y_F + q_1x_F - p_1y_E - q_1x_E] \rightarrow -\frac{1}{p_1}(p_1y_E + q_1x_E)$ as $\epsilon \rightarrow 0$. Note

that $-\frac{1}{p_1}(p_1y_E+q_1x_E) < 0$, therefore we get $y_F+\frac{q_1}{p_1}x_F < y_E+\frac{q_1}{p_1}x_E$ as $\epsilon \to 0$.

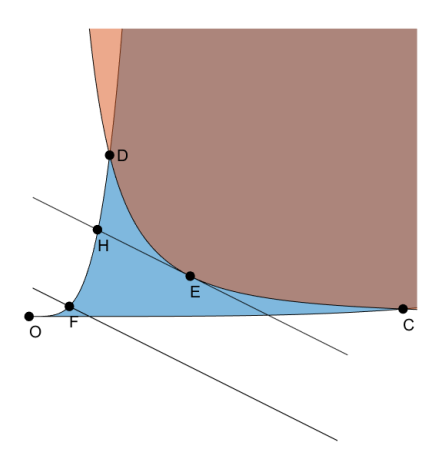


FIGURE 9. In the same setting as in Fig. 8, we now focus on relative positions of some important attracting directions lines. The point F is chosen such that the slope of the tangent line to the curve OD at F is the same as the slope of the attraction direction of the red uncertainty region.

Given the cone formed by the attracting directions in region EHD, the trajectory always remains in the region EHD. Note that the slope of the tangents to the upper blue curve increases monotonically from O to D, the red attracting direction will point towards the interior of the region R_{CD} from F to D. Suppose that the trajectory meets the curve OD at the point P'. Since y_F is lesser than the y-coordinate of the point H, we get that the red attracting direction will point towards the interior of the region R_{CD} from H to D. In particular, at P', the vector field points towards the interior of the region R_{CD} . As a consequence, the trajectory cannot cross OD.

We now prove that there exists trajectories from A to D and from B to C which stay inside the regions R_{AD} and R_{BC} respectively. Note that the slope of the tangents to the upper blue curve at A and D given by $m_A^{p_1,q_1}$ and $m_D^{p_1,q_1}$ satisfy $m_A^{p_1,q_1}\to\infty$ and $m_D^{p_1,q_1}\to\infty$ as $\epsilon\to 0$. Further, the slope of the tangents to the upper blue curve increase monotonically from D to A. For contradiction, assume that the trajectory from A to D intersects the curve AD at point P. Then the vector field at point P is given by the attracting direction corresponding to the lower red curve, which points towards the interior of the region R_{AD} .

Note that inside the region R_{AD} , the trajectory from A to D is confined to the relevant cone formed by the attracting directions of the uncertainty regions. Therefore the trajectory cannot intersect the upper red curve from A to above it. We now show that the trajectory also cannot intersect the lower red curve from D to upwards. Further, the slopes of the tangents

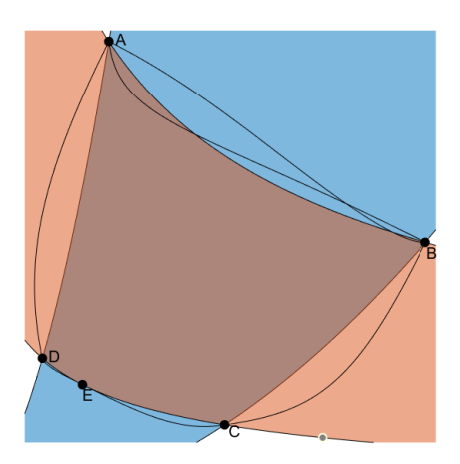


FIGURE 10. Boundary of \mathcal{M}_{ϵ} for subcase(a) in cases (v)-(vi).

to the lower red curve decrease monotonically from D to upwards. For contradiction, assume that the trajectory from A to D intersects the lower red curve from D to upwards at point P'. The vector field at P' is given by the blue attracting direction, which points towards the region R_{AD} . A similar argument can be made to show that the trajectory from B to C stays inside the region R_{BC} .

We now show how to construct the boundary of \mathcal{M}_{ϵ} in the region R_{AB} . Note that the slopes of the tangents to upper red curve satisfy $m_A^{p_2,q_2} \rightarrow$ $-\infty$ and $m_R^{p_2,q_2} \to 0$ as $\epsilon \to 0$. Consider the two trajectory that starts at A and ends at B and the trajectory that starts at B and ends at A. We will consider the outer union of these trajectories. We show that the intersection of these two trajectories cannot lie in the region ABCD. Note that in the limit $\epsilon \to 0$, on the curve AB, the slope of the tangent changes continuously on the interval $(-\infty,0)$. The blue attracting direction has a fixed negative slope given by $-\frac{p_1}{q_1}$. Therefore, both trajectories from the point A to the point B and from the point B to the point A will enter the blue uncertainty region. Let us assume that they intersect at point M. We will show that the trajectories AM and MB will form a part of the boundary of \mathcal{M}_{ϵ} . To show this, we will prove that the point M lies outside the region ABCD. The trajectories from A to B and from B to A are initially both outside the region ABCD. To enter the region ABCD, we need the slope of the tangent to the upper red curve to be greater than $-\frac{p_1}{q_1}$ for the trajectory from A to B, and to be $<-\frac{p_1}{q_1}$ for the trajectory from B to A. Since this cannot be achieved simultaneously, the intersection of the trajectories AB and BA cannot be inside the region ABCD.

(b) $p_1 + p_2 - q_1 - q_2 > 0$. In this case, we have from Table 1, $m_A^{p_1,q_1} \to \infty, m_A^{p_2,q_2} \to -\infty, m_B^{p_1,q_1} \to \infty, m_B^{p_2,q_2} \to -\infty, m_C^{p_1,q_1} \to 0, m_C^{p_2,q_2} \to 0, m_D^{p_1,q_1} \to 0, m_D^{p_2,q_2} \to 0$ as $\epsilon \to 0$. This is analogous to the subcase (a) and we can show that for ϵ small enough, the boundary of \mathcal{M}_{ϵ} is given by the following trajectories:

- 1. From A to B.
- 2. There exists a point E on the curve BC such that the slope of the tangent to the blue curve has the same slope as the attracting direction of the red uncertainty region. Now construct trajectories from E to B and E to C.
- 3. From C to D.
- 4. Outer union of the trajectories from A to D and D to A.
- (c) $p_1 + p_2 q_1 q_2 = 0$, this will be a combination of the previous situations. From Table 1, we have the following: $m_B^{p_1,q_1}=m_D^{p_1,q_1}=\frac{p_1}{q_1}$ and $m_B^{p_2,q_2}=m_D^{p_2,q_2}=rac{p_2}{q_2}$. Let E be a point on the lower red curve CDsuch that the tangent at E has the same slope as the blue attracting direction, and E' be a point on the upper red curve AB such that the tangent at E' has the same slope as the blue attracting direction. Let us assume that the slope of the tangent on the lower red curve at point C is k. Note that the slopes of the tangents decrease monotonically on the curve CD in the range $[k, \frac{p_2}{q_2}]$. Similarly, on the upper curve AB, the slopes of the tangents decrease monotonically in the range $[\frac{p_2}{q_2}, \frac{\lambda}{k}]$, where λ is some positive constant. Therefore, there is at most one point E or E' on the red curves AB or CD. When ϵ is small enough, we can construct the boundary of \mathcal{M}_{ϵ} , where the upper trajectory between A and B is like case (a) while the lower trajectory between C and D is like case (b); or the upper trajectory between A and B is like case (b) while the lower trajectory between C and D is like case (a). Similarly on the blue curves AD and BC, we have at most one special point F or F', where the slope of the tangent is same as the slope of the red attracting direction. The construction of the boundary of \mathcal{M}_{ϵ} then proceeds in identical fashion as described above.

Theorem 4.3. For small enough ϵ , the set \mathcal{M}_{ϵ} is the minimal invariant region of $\mathcal{G}_{\epsilon}^{\text{variable-k}}$.

Proof. The proof proceeds in identical fashion to Proposition 2 and Theorem 4.2. \Box

In what follows next, we show that for ϵ small enough, \mathcal{M}_{ϵ} is also the minimal globally attracting region. Towards this, we need to analyze the points amongst (A, B, C, D), that are end points of trajectories which form the boundary of \mathcal{M}_{ϵ} . In particular, for every $\epsilon > 0$, we are interested in the angle that the trajectories that form the boundary of \mathcal{M}_{ϵ} make when they meet at the globally attracting points. To make this analysis work, it is useful to linearize the dynamical system and study the eigenvalues of the corresponding Jacobian. The next proposition makes this precise.

The Jacobian corresponding to the dynamical system (10) is given by $J=\begin{pmatrix} J_{11} & J_{12} \\ J_{21} & J_{22} \end{pmatrix}$ where

$$J_{11} = (a'_1 - a_1)a_1k_1x^{a_1 - 1}y^{b_1} - (a'_1 - a_1)a'_1k_2x^{a'_1 - 1}y^{b'_1}$$

$$+ (a'_2 - a_2)a_2k_3x^{a_2 - 1}y^{b_2} - (a'_2 - a_2)a'_2k_4x^{a'_2 - 1}y^{b'_2}.$$

$$J_{12} = (a'_1 - a_1)b_1k_1x^{a_1}y^{b_1 - 1} - (a'_1 - a_1)b'_1k_2x^{a'_1}y^{b'_1 - 1}$$

$$+ (a'_2 - a_2)b_2k_3x^{a_2}y^{b_2 - 1} - (a'_2 - a_2)b'_2k_4x^{a'_2}y^{b'_2 - 1}.$$

$$J_{21} = (b'_1 - b_1)a_1k_1x^{a_1 - 1}y^{b_1} - (b'_1 - b_1)a'_1k_2x^{a'_1 - 1}y^{b'_1}$$

$$+ (b'_2 - b_2)a_2k_3x^{a_2 - 1}y^{b_2} - (b'_2 - b_2)a'_2k_4x^{a'_2 - 1}y^{b'_2}.$$

$$J_{22} = (b'_1 - b_1)b_1k_1x^{a_1}y^{b_1 - 1} - (b'_1 - b_1)b'_1k_2x^{a'_1}y^{b'_1 - 1}$$

$$+ (b'_2 - b_2)b_2k_3x^{a_2}y^{b_2 - 1} - (b'_2 - b_2)b'_2k_4x^{a'_2}y^{b'_2 - 1}.$$

$$(21)$$

Proposition 4. Consider case (i) and the trajectory from D to A. (A similar analysis will apply to other cases). Let $J = \begin{pmatrix} J_{11} & J_{12} \\ J_{21} & J_{22} \end{pmatrix}$ be the Jacobian corresponding to the linearized dynamical system of this trajectory at point A. As ϵ varies, J can only have equal eigenvalues at finitely many points.

Proof. Note that for J to have equal eigenvalues, it has to satisfy

$$(J_{11} + J_{22})^2 = 4(J_{11}J_{22} - J_{12}J_{21}) (22)$$

From Lemma 4.1, the point A is the intersection of the following curves

$$\frac{1}{\epsilon} x^{a'_1} y^{b'_1} = \epsilon x^{a_1} y^{b_1}
\epsilon x^{a_2} y^{b_2} = \frac{1}{\epsilon} x^{a'_2} y^{b'_2}$$
(23)

Solving Equations (22) and (23), we get a quasi-polynomial equation in ϵ , which has finitely many roots. Therefore, the number of points where J has equal eigenvalues are finite.

The next proposition says that for trajectories that form the boundary of \mathcal{M}_{ϵ} , certain directions are forbidden.

Proposition 5. Consider case (i) and the trajectory from D to A. (A similar analysis will apply to other cases). Let $J = \begin{pmatrix} J_{11} & J_{12} \\ J_{21} & J_{22} \end{pmatrix}$ be the Jacobian corresponding to the linearized dynamical system of this trajectory at point A. Then the trajectory approaches the point A along the slower (smaller in magnitude) eigendirection of the Jacobian J.

Proof. Note that the trajectory approaches the point A along the slower(smaller in magnitude) eigendirection unless it lies on the faster (larger in magnitude) eigendirection. We show that the trajectory cannot approach the point A along the faster eigendirection. In particular, we show that the faster eigendirection lies in the second or fourth quadrant centred at A (refer to Figure 6), which is forbidden by Proposition 1.

It is known [11, Theorem 14.3.4] that given a detailed balanced dynamical system with a positive steady state c^* , the Jacobian is symmetric with respect to the inner product given by $u*w=\frac{u_1w_1}{c_1^*}+\frac{u_2w_2}{c_2^*}$. There is a change of basis transformation that takes the Jacobian J in the standard basis to the Jacobian J^* that is symmetric with respect to this inner product, given by $J^*=P^{-1}JP$ where $P=\begin{pmatrix} \sqrt{c_1^*} & 0 \\ 0 & \sqrt{c_2^*} \end{pmatrix}$ Note that signs of each element of J is unchanged by this transformation. Using Lemma 4.1 and the Jacobian given by Equation (21), the off-diagonal elements J_{12}

and J_{21} of the Jacobian at A are given by the following

- $\bullet \ \ J_{12}=(a_1'-a_1)b_1\frac{1}{\epsilon}x^{a_1}y^{b_1-1}-(a_1'-a_1)b_1'\epsilon x^{a_1'}y^{b_1'-1}+(a_2'-a_2)b_2\frac{1}{\epsilon}x^{a_2}y^{b_2-1}-$
- $(a'_2 a_2)b'_2 \epsilon x^{a'_2} y^{b'_2 1}.$ $J_{21} = (b'_1 b_1)a_1 \frac{1}{\epsilon} x^{a_1 1} y^{b_1} (b'_1 b_1)a'_1 \epsilon x^{a'_1 1} y^{b'_1} + (b'_2 b_2)a_2 \frac{1}{\epsilon} x^{a_2 1} y^{b_2} (b'_2 b_2)a'_2 \epsilon x^{a'_2 1} y^{b'_2}$

At point A, we have $\frac{1}{\epsilon}x^{a_1}y^{b_1} = \epsilon x^{a'_1}y^{b'_1}$ and $\frac{1}{\epsilon}x^{a_2}y^{b_2} = \epsilon x^{a'_2}y^{b'_2}$. Since we are in case (i), we have $(a'_1-a_1)(b_1-b'_1)>0$ and $(a'_2-a_2)(b_2-b'_2)>0$. Therefore, we get $J_{12}>0$ and $J_{21} > 0$. This implies that $J_{12}^* = J_{21}^* > 0$. The eigenvector corresponding to the

smaller eigenvalue for a symmetric 2×2 matrix is given by $e_1 = \begin{pmatrix} \frac{J_{11}^* - J_{22}^* - \Delta}{2J_{12}^*} \\ 1 \end{pmatrix}$ where

 $\Delta = \sqrt{(J_{11}^* - J_{22}^*)^2 + 4{J^*}_{12}^2}. \text{ Since } \frac{J_{11}^* - J_{22}^* + \Delta}{2J_{12}^*} < 0, \text{ this eigenvector points either in the second or fourth quadrant. Transforming this eigenvector to the standard basis}$ using $P^{-1}e_1$ does not change the sign of the elements of the eigenvector. Therefore, the vector corresponding to the faster eigendirection lies either in the second or fourth quadrant centred at A, and we are done.

Theorem 4.4. For small enough ϵ , the set \mathcal{M}_{ϵ} is a globally attracting region of $\mathcal{G}_{\epsilon}^{\text{variable-k}}$.

Proof. Let ϵ_0 be small enough so that the region \mathcal{M}_{ϵ_0} can be constructed according to the procedure described in Section 4.1. Note that \mathcal{M}_{ϵ} varies continuously as a function of ϵ . In addition, we have $\bigcup_{\epsilon \in (0,\epsilon_0]} \mathcal{M}_{\epsilon} = \mathbb{R}^2_{>0}$. Let ζ be small enough so

that the region $\mathcal{M}_{\epsilon_0+\zeta}$ can still be constructed. Let $\boldsymbol{x}(t)$ be a solution of $\mathcal{G}^{\text{variable-k}}_{\epsilon}$ with $\boldsymbol{x}(0) \in \mathbb{R}^2_{>0}$. Since $\bigcup \mathcal{M}_{\epsilon+\zeta} = \mathbb{R}^2_{>0}$, one can choose ϵ_1 with $0 < \epsilon_1 < \epsilon_0$

 \bigcup \mathcal{M}_{ϵ} . We will prove that $\boldsymbol{x}(t) \in \mathcal{M}_{\epsilon_0}$ for a large enough such that $x(0) \in$

Towards this, let $\partial \mathcal{M}_{\epsilon}$ denote the boundary of \mathcal{M}_{ϵ} . Define a function Γ : $\bigcup_{\{\epsilon_0, \epsilon_1, \epsilon_2\}} \partial \mathcal{M}_{\epsilon} \to \left[\frac{1}{\epsilon_0 + \zeta}, \frac{1}{\epsilon_1}\right] \text{ so that } \Gamma(x, y) = \frac{1}{\epsilon} \text{ if } (x, y) \in \mathcal{M}_{\epsilon}. \text{ We will show } \Gamma(x, y) = \frac{1}{\epsilon} \left[\frac{1}{\epsilon_0 + \zeta}, \frac{1}{\epsilon_1}\right] = \frac{1}{\epsilon} \left[\frac{1}{\epsilon_0 + \zeta}, \frac{1}{\epsilon_1}\right]$

that $\Gamma(\boldsymbol{x}(t)) \leq \frac{1}{\epsilon_0}$ for a large enough t. Let us assume that this is not true. By

Proposition 2, we know that the sets $\Gamma^{-1}\left(0,\frac{1}{\epsilon_0}\right] = \mathcal{M}_{\epsilon_0}$ and $\Gamma^{-1}\left(0,\frac{1}{\epsilon_1}\right] = \mathcal{M}_{\epsilon_1}$ are invariant. This implies that $\Gamma(\boldsymbol{x}(t)) \in \left[\frac{1}{\epsilon_0},\frac{1}{\epsilon_1}\right]$ for all $t \geq 0$.

Note that the function Γ is differentiable everywhere executive.

Note that the function Γ is differentiable everywhere except maybe on boundary of \mathcal{M}_{ϵ} , where trajectories end or where trajectories can start or intersect. We will handle these cases separately. We will denote the curve that contains such points where Υ is not differentiable by $C_i(\epsilon)$.

Case I. Consider points on the boundary of \mathcal{M}_{ϵ} where trajectories can start or intersect. Note that in this case, the angle made by \mathcal{M}_{ϵ} along C_j is always greater than π no matter what ϵ is (this follows from analyzing cases (v) and (vi)). We will use some machinery from convex analysis. Towards this, for each curve C_j , let Υ_{i1} and Υ_{i2} be two functions such that $\Upsilon = \Upsilon_1$ on one side of C_i and $\Upsilon =$ Υ_2 on the other side. We now consider the following cases. We let $-\Upsilon(x)=$ $\max(-\Upsilon_{j1}(\boldsymbol{x}), -\Upsilon_{j2}(\boldsymbol{x}))$ in a neighbourhood of the curve C_j . Defining $\Upsilon(\boldsymbol{x})$ this way ensures that $\Upsilon(x)$ is lower C^1 [17, 16]. The subgradient of $\Upsilon(x)$ along $C_i(\epsilon)$ is given by

$$\partial \Upsilon(\mathbf{x}) = \{ \gamma \nabla \Upsilon_{j1}(\mathbf{x}) + (1 - \gamma) \Upsilon_{j2}(\mathbf{x}) \mid \gamma \in [0, 1] \}. \tag{24}$$

Using the continuity of Υ , we can apply the chain rule of gradients [17, Theorem 10.6] to get

$$\partial(\Upsilon \circ \boldsymbol{x})(t) \subset \{\boldsymbol{z} \cdot \dot{\boldsymbol{x}}(t) \,|\, \boldsymbol{z} \in \partial \Upsilon(\boldsymbol{x}(t))\}. \tag{25}$$

Note that Proposition 2 shows that \mathcal{M}_{ϵ} is invariant, i.e., the vector field along its boundary points towards the interior of \mathcal{M}_{ϵ} . Consider a compact neighbourhood \mathcal{K} of the curve C_j . Since \mathcal{K} is compact, there is a $\delta > 0$ such that $\dot{\boldsymbol{x}} \cdot \nabla \Upsilon_{j1} < -\delta$ and $\dot{\boldsymbol{x}} \cdot \nabla \Upsilon_{j2} < -\delta$ on \mathcal{K} . From (24), we get that there exists a $\delta > 0$ such that $\boldsymbol{z} \cdot \dot{\boldsymbol{x}}(t) < -\delta < 0$ for all $\boldsymbol{z} \in \partial \Upsilon(\boldsymbol{x}(t))$ in \mathcal{K} . Using (25), we get

$$\sup_{t \ge 0} \partial (\Upsilon \circ \boldsymbol{x})(t) < -\delta. \tag{26}$$

Since Υ is lower C^1 , one can apply the mean value theorem [17, Theorem 10.48] to $\Upsilon \circ \boldsymbol{x}(t)$ to get that there is a $\tau \in [0, t]$

$$\Upsilon(\boldsymbol{x}(t)) - \Upsilon(\boldsymbol{x}(0)) = t\alpha_t \text{ for some } \alpha_t \in \partial(\Upsilon \circ \boldsymbol{x})(\tau).$$
 (27)

Since $\alpha_t < \delta$, this implies that on \mathcal{K} , we have

$$\Upsilon(\mathbf{x}(t)) < \Upsilon(\mathbf{x}(0)) - \delta t \tag{28}$$

for all t > 0. This contradicts the fact that $\Upsilon(\boldsymbol{x}(t)) \in [\frac{1}{\epsilon_0}, \frac{1}{\epsilon_1}]$ for all t > 0.

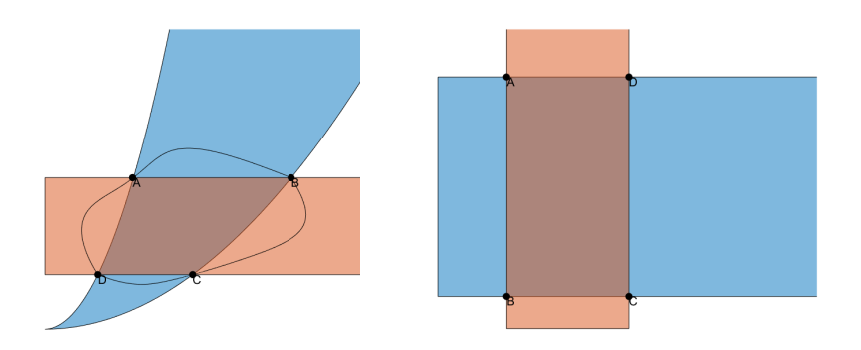
Case II. Consider points on the boundary of \mathcal{M}_{ϵ} that are end points of trajectories. In this case, the angle made by \mathcal{M}_{ϵ} along C_j can be equal to or different from π depending on whether the eigenvalues of the Jacobian are equal or not. From Proposition 4, we know that the set of points when the eigenvalues of the Jacobian are equal is finite. Let $(\epsilon_1, \epsilon_2,, \epsilon_k)$ be the set such that for each ϵ_i in $(\epsilon_1, \epsilon_2,, \epsilon_k)$, the boundary of \mathcal{M}_{ϵ_i} contains end points of trajectories where the Jacobian has equal eigenvalues. For each such ϵ_i , contruct a small enough annular region around \mathcal{M}_{ϵ_i} . Note that since the annular region is a compact set, by continuity there exists a δ_0 such that $\dot{x} \cdot \Delta \Upsilon < -\delta_0$. Between the annular regions, the function $\Upsilon(x)$ is C^1 . Therefore there exists a δ_1 such that $\dot{x} \cdot \Delta \Upsilon < -\delta_1$. Therefore, we have $\dot{x} \cdot \Delta \Upsilon < \min(-\delta_0, -\delta_1)$. We can now repeat the procedure as in Case I to get our desired conclusion. The only case that remains to be resolved when we have distinct eigenvalues is when we start along the faster eigen direction. However, this case does not occur due to Proposition 5.

Theorem 4.5. For small enough ϵ , the set \mathcal{M}_{ϵ} is the minimal globally attracting region of $\mathcal{G}_{\epsilon}^{\text{variable-k}}$.

Proof. Theorem 4.4 shows that \mathcal{M}_{ϵ} is a globally attracting region. We now show that it is the minimal globally attracting region, i.e., it is contained in every globally attracting region. Towards this, consider a an arbitrary point $Q \in \mathcal{M}_{\epsilon}$. We will show that Q lies in the omega-limit point of some trajectory of $\mathcal{G}^{\text{variable-k}}_{\epsilon}$. Consider $P_2 \in \mathcal{M}_{\epsilon}$ such that $P_2 \neq Q$. From Proposition 3, we have $P_1 \leadsto P_2$ for any $P_1 \in \mathbb{R}^2_{>0}$. Choose some $\eta_1 > 0$. Then there exists a time t_1 and trajectory $\boldsymbol{x}(t)$ with $\boldsymbol{x}(0) = P_2$ such that $||\boldsymbol{x}(t_1) - Q|| < \eta_1$. Choose $\eta'_1 > 0$. Using Proposition 3 again, we get that there exists a time $t'_1 > t_1$ and a trajectory starting at $\boldsymbol{x}(t_1)$ such that $||\boldsymbol{x}(t'_1) - P_2|| < \eta'_1$. Now choose $\eta_2 > 0$ such that $\eta_2 < \eta_1$. Using Proposition 3 again, we get that there exists a time $t_2 > t'_1$ and trajectory starting at $\boldsymbol{x}(t'_1)$ such that $||\boldsymbol{x}(t'_2) - Q|| < \eta_2$. Repeating this procedure generates a trajectory $\boldsymbol{x}(t)$ and

a sequence $\eta_1 > \eta_2 > ... > \eta_k$ such that $\lim_{k \to \infty} \eta_k = 0$ and a sequence of times $t_1 < t_2 < ... < t_k$ such that $\lim_{k \to \infty} t_k = \infty$ and $\lim_{k \to \infty} \boldsymbol{x}(t_k) = Q$. This implies that Q lies in the omega-limit of this trajectory.

- 5. **Special cases.** The goal of this section is to handle the special cases that we have *not* considered in our analysis so far. More precisely, these are: (i) dynamical systems corresponding to two reversible reactions with conservation laws, (ii) dynamical systems corresponding to two reversible reactions, where one of the reaction vectors is parallel to an axis, and (iii) dynamical systems corresponding to two reversible reactions, where both reaction vectors are parallel to the axes. We present their analysis below:
 - 1. Dynamical systems corresponding to two reversible reactions with conservation laws: The analysis for this case is similar to the case when there is only one reaction. The minimal invariant region and the minimal globally attracting region \mathcal{M}_{ϵ} in this cases is exactly as given in Remark 1.
 - 2. Dynamical systems corresponding to two reversible reactions, where one of the reaction vectors is parallel to an axis: A typical depiction of the uncertainty regions in this case is shown in Figure 11a. The analysis is identical to cases (i)-(iv) discussed in Section 3. In particular, the boundary of \mathcal{M}_{ϵ} is generated by trajectories starting from points B and D and existing at points A and C as shown in Figure 11a. The region enclosed by this boundary is the minimal invariant region and the minimal globally attracting region \mathcal{M}_{ϵ} .



- (A) Uncertainty regions corresponding to two reversible reactions, ing to two reversible reactions, where one of the reaction vectors is where both reaction vectors are parparallel to an axis. The set \mathcal{M}_{ϵ} is allel to the axes. The set \mathcal{M}_{ϵ} is the also shown.
- 3. Dynamical systems corresponding to two reversible reactions, where both the reaction vectors are parallel to the axes: The uncertainty regions in this case are depicted in Figure 11b. The minimal invariant region and the minimal globally attracting region \mathcal{M}_{ϵ} is given by the intersection of the two uncertainty regions, which is a rectangle as depicted in Figure 11b.

6. **Discussion.** In this paper, we have constructed minimal invariant regions and minimal globally attracting regions for variable-k dynamical systems generated by networks possessing two reversible reactions. In this special case, the minimal invariant region coincides with the minimal globally attracting region. Of course, these regions are also invariant and globally attracting regions for the corresponding fixed-k mass-action systems.

In previous work [10] we have constructed minimal invariant regions and minimal globally attracting regions for general toric differential inclusions [7, 4] in two dimensions. Therefore, since large classes of mass-action systems can be embedded [6, 5] into toric differential inclusions, this provides some invariant regions and some globally attracting regions (but not necessarily minimal ones) for many variable-k and fixed-k mass-action systems with any number of reactions, even if they are not reversible, as long as they can be embedded into toric differential inclusions. In particular, this applies to all weakly reversible and to all endotactic networks in two dimensions.

We have only considered here variable-k dynamical systems with two reversible reactions; this is the simplest nontrivial case for this class of problems, and we regard the results obtained here as a proof-of-concept for future work in this area. Numerical simulations suggest that the analysis of the more general case with arbitrary number of reversible reactions can be significantly more complicated. Similarly, numerical simulations for the construction of minimal invariant regions and minimal globally attracting regions for fixed-k dynamical systems suggest that this problem might also be quite difficult, in general. We think that these are very interesting avenues for future work.

Acknowledgments. G.C. and Y.D. would like to acknowledge support from NSF grants DMS-1816238 and DMS-2051568. A.D. would like thank the Mathematics Department at University of Wisconsin-Madison for a Van Vleck Visiting Assistant Professorship.

REFERENCES

- L. Adleman, M. Gopalkrishnan, M. Huang, P. Moisset and D. Reishus, On the mathematics of the law of mass action, in A Systems Theoretic Approach to Systems and Synthetic Biology I: Models and System Characterizations, Springer, 2014, 3–46.
- [2] D. Anderson, A proof of the global attractor conjecture in the single linkage class case, SIAM J. Appl. Math., 71 (2011), 1487–1508.
- [3] F. Blanchini, Set invariance in control, Automatica, 35 (1999), 1747–1767.
- [4] G. Craciun, Toric differential inclusions and a proof of the global attractor conjecture, arXiv preprint, arXiv:1501.02860.
- [5] G. Craciun, Polynomial dynamical systems, reaction networks, and toric differential inclusions, SIAM J. Appl. Algebra Geom., 3 (2019), 87–106.
- [6] G. Craciun and A. Deshpande, Endotactic networks and toric differential inclusions, SIAM J. Appl. Dyn. Syst., 19 (2020), 1798–1822.
- [7] G. Craciun, A. Deshpande and H. J. Yeon, Quasi-toric differential inclusions, Discrete Contin. Dyn. Syst. Ser. B, 26 (2021), 2343–2359.
- [8] G. Craciun, A. Dickenstein, A. Shiu and B. Sturmfels, Toric dynamical systems, J. Symbol. Comput., 44 (2009), 1551–1565.
- [9] G. Craciun, F. Nazarov and C. Pantea, Persistence and permanence of mass-action and power-law dynamical systems, SIAM J. Appl. Math., 73 (2013), 305–329.
- [10] Y. Ding, A. Deshpande and G. Craciun, Minimal invariant regions and minimal globally attracting regions for toric differential inclusions, Adv. in Appl. Math., 136 (2022), Paper No. 102307, 34 pp. arXiv:2006.08735.
- [11] M. Feinberg, Foundations of Chemical Reaction Network Theory, Springer, 2019.

- [12] M. Gopalkrishnan, E. Miller and A. Shiu, A geometric approach to the global attractor conjecture, SIAM J. Appl. Dyn. Sys., 13 (2014), 758-797.
- [13] J. Gunawardena, Chemical reaction network theory for in-silico biologists, Notes available for download at http://vcp.med.harvard.edu/papers/crnt.pdf, 5.
- [14] M. Nagumo, Über die Lage der integralkurven gewöhnlicher Differentialgleichungen, Proceedings of the Physico-Mathematical Society of Japan. 3rd Series, 24 (1942), 551–559.
- [15] C. Pantea, On the persistence and global stability of mass-action systems, SIAM J. Math. Anal., 44 (2012), 1636–1673.
- [16] R. T. Rockafellar, Convex Analysis, Princeton University Press, Princeton, NJ. 1970.
- [17] R. Rockafellar and R. Wets, Variational Analysis, vol. 317, Springer Science & Business Media, 2009.
- [18] M. Savageau, Biochemical systems analysis: I. Some mathematical properties of the rate law for the component enzymatic reactions, J. Theor. Biol., 25 (1969), 365–369.
- [19] D. Siegel and D. MacLean, Global stability of complex balanced mechanisms, J. Math. Chem., 27 (2000), 89–110.
- [20] E. D. Sontag, Structure and stability of certain chemical networks and applications to the kinetic proofreading model of T-cell receptor signal transduction, *IEEE Transactions on Automatic Control*, 46 (2001), 1028–1047.
- [21] E. Voit, H. Martens and S. Omholt, 150 years of the mass action law, PLoS Comput. Biol., 11 (2015), e1004012.
- [22] P. Waage and C. Gulberg, Studies concerning affinity, J. Chem. Edu., 63 (1986), 1044.
- [23] P. Yu and G. Craciun, Mathematical analysis of chemical reaction systems, Isr. J. Chem., 58 (2018), 733–741.

Received November 2021; revised May 2022; early access July 2022.

E-mail address: yidading@outlook.com

E-mail address: abhishek.deshpande@iiit.ac.in

E-mail address: craciun@wisc.edu